Postfusional regulation of cleft glutamate concentration during LTP at 'silent synapses'

Sukwoo Choi[1], Jürgen Klingauf[1,2] and Richard W. Tsien[1]

[1] *Department of Molecular and Cellular Physiology, Beckman Center, Stanford University School of Medicine, Stanford, California 94305-5345, USA*

[2] *Present address: Max-Planck Institute for Biophysical Chemistry, Dept. Membrane Biophysics, Am Fassberg 11 37077 Göttingen, Germany*

Correspondence should be addressed to R.W.T. (rwtsien@leland.stanford.edu)

'Silent synapses' show responses from high-affinity NMDA receptors (NMDARs) but not low-affinity AMPA receptors (AMPARs), but gain AMPAR responses upon long-term potentiation (LTP). Using the rapidly reversible NMDAR antagonist L-AP5 to assess cleft glutamate concentration ($[glu]_{cleft}$), we found that it peaked at <<170 μM at silent neonatal synapses, but greatly increased after potentiation. Cyclothiazide (CTZ), a potentiator of AMPAR, revealed slowly rising AMPA EPSCs at silent synapses; LTP shortened their rise times. Thus, LTP at silent synapses increased rate-of-rise and peak amplitude of $[glu]_{cleft}$. Release probability reported by NMDARs remained unchanged during LTP, implying that $[glu]_{cleft}$ increases arose from immediately presynaptic terminals. Our data suggest that changes in the dynamics of fusion-pore opening contribute to LTP.

Activity-dependent changes in synaptic efficacy such as LTP and long-term depression (LTD) are thought to be important for information storage and the appropriate development of neural circuitry in the brain. Although there is progress in understanding mechanisms of LTP expression, considerable controversy remains[1–3]. One important observation, widely replicated at various central synapses[4–6], is that a proportion of glutamatergic synaptic connections show no AMPAR-mediated currents, but clear NMDAR-mediated currents, particularly upon strong postsynaptic depolarization. These 'silent synapses' can become fully functional upon induction of LTP[4–6]. A popular hypothesis to account for this conversion of silent synapses invokes a postsynaptic mechanism whereby silent synapses lacking functionally active AMPARs somehow gain them as a result of the potentiation. A proportion of synapses (<20%) show no significant labeling by anti-AMPAR antibodies[7], and fluorescently tagged AMPARs can undergo externalization during the course of LTP[8]. None of the evidence for postsynaptic changes precludes the possibility of concomitant changes in presynaptic function; postsynaptic and presynaptic mechanisms are not mutually exclusive. Indeed, there is compelling cell-biological evidence in hippocampal cultures that LTP is associated with *bona fide* changes in presynaptic function, as monitored by presynaptic uptake of membrane-impermeable antibodies[9] or FM dyes[10,11]. These studies establish that, in principle, nerve terminals are capable of enhancing turnover or accessibility of vesicles upon potentiation.

Any putative presynaptic mechanism must be compatible with the finding that NMDAR responses are little changed at the time that AMPAR events are greatly enhanced. Because NMDARs and AMPARs have widely different affinities for glutamate[12], it is possible that small but slow transients in $[glu]_{cleft}$ would strongly activate high-affinity NMDA receptors but not low-affinity AMPA receptors[12–15]. Such transients in $[glu]_{cleft}$ could arise from diffusional spread of neurotransmitter released from neighboring terminals ('spillover')[16], or by a nonexpanding opening of the presynaptic fusion pore, as previously decribed in leech neurons[17] and non-neuronal secretory cells[18–20]. In either case, the prediction is that LTP involves an increase in $[glu]_{cleft}$.

We assessed $[glu]_{cleft}$ in two ways. First, we monitored the blockade of NMDAR responses with a rapidly reversible antagonist, L-AP5 (refs. 21,22), and second, we examined AMPAR-mediated synaptic events in the presence of an AMPAR potentiator, cyclothiazide. The results indicate that $[glu]_{cleft}$ at 'silent synapses' sharply increased with LTP, and that 'silent synapses' actually contained an appreciable number of AMPA receptors.

Results

To assess the peak $[glu]_{cleft}$ at 'silent synapses', we used a pharmacological approach that relied on a rapidly unbinding antagonist for NMDARs[21,22]. The method is based on the principle that the degree of antagonist inhibition depends upon the peak transmitter concentration during neurotransmission: the higher $[glu]_{cleft}$, the less the inhibition. We chose L-AP5 ($K_i \approx 40$ μM)[23] as the low-affinity antagonist because its off-rate is faster than for other available NMDA antagonists (such as D-α-diaminoadipate[21,22,24]). Using a piezoelectric device to exchange solutions quickly, we assessed the kinetics of L-AP5 binding and unbinding in outside-out patch recordings of NMDA currents. We first tested whether 250 μM L-AP5 ($>>K_i$) was sufficient to occupy almost all the NMDARs in the absence of glutamate (**Fig. 1a**). In the continuous presence of 250 μM L-AP5, pulses (1 ms) of 50 μM glutamate produced only 3.4 ± 1.8% of the current induced by the same glutamate application without antagonist ($n = 5$). Thus, >95% of receptors were occupied by L-AP5. Second, we assessed the unbinding rate of L-AP5 by monitoring antagonist unblock during the application of a saturating concentration of glutamate (5 mM). In the continuous

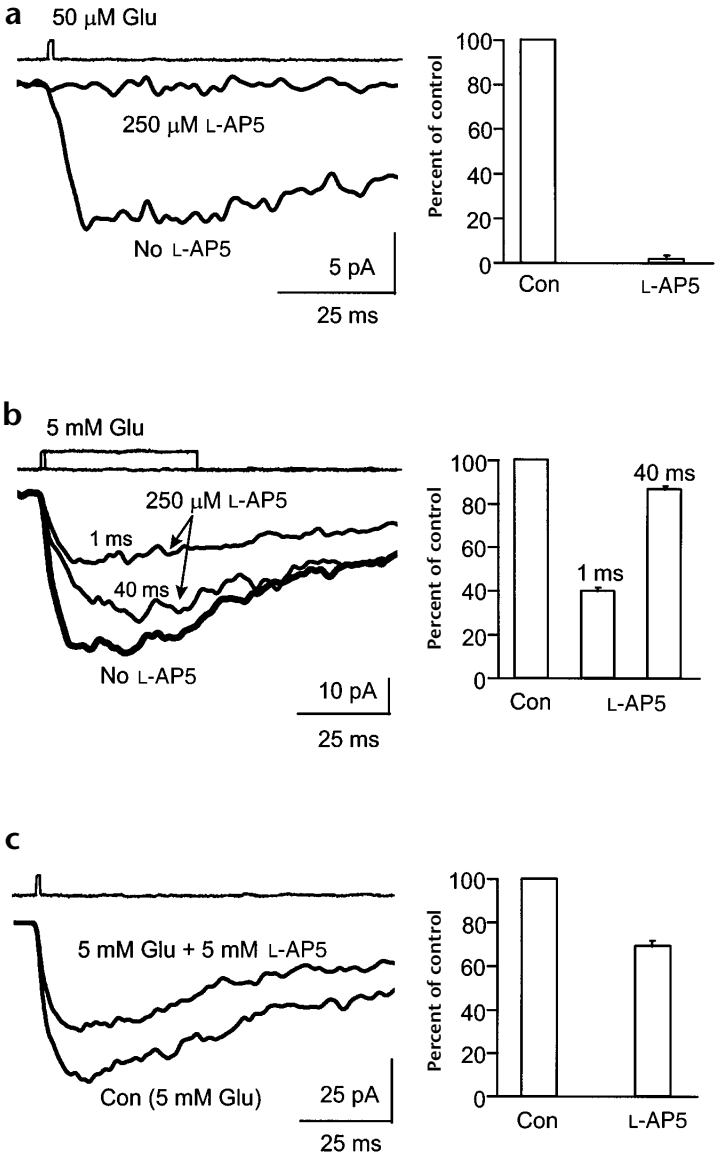

Fig 1. Binding and unbinding kinetics of L-AP5 on NMDA receptors in outside-out patches. (**a**, left) Current records showing averaged responses to 1-ms pulses of 50 μM glutamate, alone or in the continuous presence of 250 μM L-AP5. (**a**, upper trace) Open-tip responses acquired after rupture of the patch. (**a**, right) Pooled data from five patches. (**b**, left) Averaged current responses to 1-ms or 40-ms pulses of 5 mM glutamate in the continuous presence of L-AP5 (250 μM). A saturating concentration of glutamate was used to block any rebinding of L-AP5 during the glutamate pulses. Heavy line indicates response to a 40-ms pulse of 5 mM glutamate in the absence of L-AP5, in the same patch. (**b**, right) Pooled data from 5 patches. In L-AP5, 1-ms pulses of glutamate produced peak currents ~40% of those in the absence of antagonist, in contrast with previous findings for D-AA (<10% of control for 1-ms pulses[15]), indicating that L-AP5 unbinds much faster than D-AA. Changes in $[glu]_{cleft}$ with D-AA would be too small to detect, as in cortical neurons[24]. (**c**) Averaged current traces showing responses to 1-ms pulses of 5-mM glutamate alone (con) or 5 mM glutamate + 5 mM L-AP5. (**c**, right) Summary of data from eight patches. Response amplitudes for glutamate + L-AP5 averaged 69.2 ± 2.5% of those for glutamate alone. In each panel, the different protocols were interleaved to minimize any possible effects of rundown.

presence of 250 μM L-AP5, 1-ms pulses of glutamate produced 40.0 ± 1.4% of the maximal control current (n = 5, **Fig. 1b**), indicating that L-AP5 can unbind from ≥40% of the NMDA receptors during a 1-ms period. Third, the on-rate for L-AP5 binding was estimated to be 1.44-fold slower than that of glutamate, based on comparisons between responses to agonist plus antagonist or to agonist alone (**Fig. 1c**), allowing for the finite duration of drug application. Fourth, we carried out experiments to address possible concerns about contamination of L-AP5 by its high affinity D-isomer[21]. As expected from the purity of the drug (<0.5% D-AP5 by HPLC, D. Hall, Tocris Cookson, personal communication), the antagonist block was almost completely relieved by prolonged glutamate application (**Fig. 1b**).

Synaptic transmission was evoked by minimal stimulation of the Schaffer collateral commissural pathway to hippocampal area CA1 (**Fig. 2**). In cases in which the stimulation evoked mixed transmission (AMPAR current at –60 mV as well as NMDAR current at +40 mV), L-AP5 blockade of NMDAR currents was always incomplete (16 of 16 cells, mean inhibition, 68.9 ± 3.7%). In contrast, at silent synapses showing no detectable AMPAR currents but clear NMDAR responses, NMDA EPSCs were almost completely inhibited by 250 μM L-AP5 (12 of 12 cells, mean inhibition, 99.7 ± 1.0%). Pairing of pre- and postsynaptic activity was successful in inducing potentiation in 6 of 12 cells; in these cases, failure of AMPAR responses sharply decreased after pairing as previously reported[4–6]. The lack of synaptic enhancement in the remaining recordings can be attributed to washout of LTP under whole-cell recording[25]. In contrast, LTP was not induced when the pairing procedure was carried out in 50 μM D-AP5 (n = 8, p < 0.004), as would be expected for NMDAR-dependent plasticity (data not shown). We tested the effects of L-AP5 on NMDAR currents at silent synapses initially lacking AMPAR currents that were converted into fully functional ones. Whereas L-AP5 reduced NMDAR currents by 99.2 ± 3.4% before pairing, the inhibition was much milder after pairing (50.2 ± 3.3%, n = 6, p < 0.001). The significant reduction in the degree of inhibition by L-AP5 indicates that the peak value of $[glu]_{cleft}$ increased along with the potentiation.

A more quantitative estimate of peak $[glu]_{cleft}$ sensed by NMDARs at postsynaptically silent synapses can be obtained on the basis of empirically derived antagonist characteristics[22]. From recordings from the outside-out patches in Fig. 1, we determined that the on-rate coefficient for L-AP5 was 1.44-fold less than for glutamate. Because complete block of channel opening can only occur if antagonist binding greatly exceeds neurotransmitter binding[22], the finding that 250 μM L-AP5 suffices to completely block transmission implies that peak $[glu]_{cleft}$ is <<250 μM/1.44, that is, <<170 μM. This upper limit is far lower than the ~2 mM estimated for conventionally active synapses[15,26], and would be expected to produce negligible activation of AMPARs, given its highly cooperative dependence on [glu][27]. Indeed, pulses of glutamate (100 μM, 1 ms) to outside-out patches produced only 1.5 ± 0.6% of the maximal AMPA current evoked by 10 mM glutamate (n = 3).

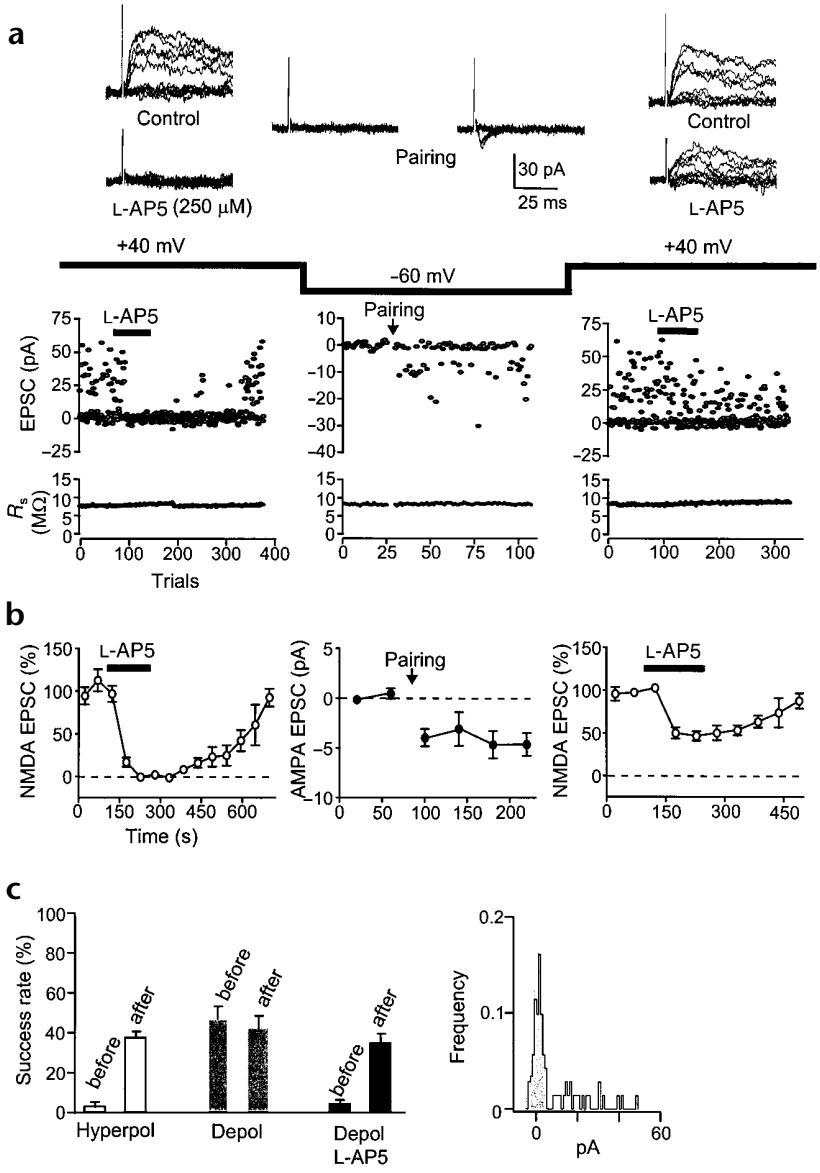

Fig. 2. L-AP5 (250 μM) completely inhibited NMDAR-mediated synaptic responses at silent synapses but lost effectiveness after pairing. (**a**, top) Representative experiment showing that the degree of inhibition of NMDA EPSCs by L-AP5 decreased during conversion of silent synapses into functional ones. EPSCs were elicited at a frequency of 0.5 Hz. (**a**, upper left, upper right) Groups of 10 consecutive NMDAR-mediated current records, taken before and after exposure to 250 μM L-AP5. (**a**, bottom) EPSC amplitude and series resistance (R_s) in the same experiment. (**b**, left) Pooled data from silent synapses before pairing, showing that 250 μM L-AP5 completely inhibited NMDA EPSCs (n = 12). We applied L-AP5 for 150 s. Pairing given within 800 s after the start of the whole-cell recording caused an immediate but stable recruitment of AMPAR responses (**b**, middle) as seen in data averaged without exclusion of failures. After pairing and successful potentiation, repeated application of L-AP5 (same concentration and duration) inhibited NMDA EPSCs to a lesser extent (right, n = 6). (**c**, left) Summary showing rate of EPSC successes (non-failures) before and after pairing in cells in which pairing induced potentiation (n = 6). The proportion of synaptic failures was estimated by doubling the fraction of responses with a less-than-zero amplitude[3]. The success rate of NMDAR EPSCs at +40 mV (shaded bars) did not change significantly during LTP ($p > 0.05$). (**c**, right) Amplitude distribution of NMDA EPSCs during exposure to 250 μM L-AP5, before pairing (shaded histogram) and after pairing (open histogram). Note that the behavior of NMDARs treated with 250 μM L-AP5 mimicked that of AMPARs at silent synapses.

If silent synapses possess AMPARs that are not activated because peak $[glu]_{cleft}$ is too low, one would expect these synapses to show AMPAR-mediated synaptic events if their glutamate affinity were enhanced. To test this idea, we used cyclothiazide, an agent known to elevate AMPAR responsiveness by increasing glutamate sensitivity[28] and inhibiting desensitization[29,30]. Initially, we carried out experiments to rule out the possibility that CTZ might have presynaptic effects, as sometimes reported[31,32] (but see ref. 28). To determine whether CTZ had any effects on transmitter release in CA1, we recorded glutamate transporter currents from astroglia in stratum radiatum as a measure of glutamate release independent of postsynaptic receptors[28,33,34] (**Fig. 3a**). THA, a selective blocker of glutamate transporters, reduced the glial currents. The glial transporter currents showed the same degree of paired-pulse facilitation (PPF) as synaptic currents, supporting their reliability as indicators of altered synaptic glutamate release[33,34]. The prominence of PPF in our glial recordings demonstrated that the glutamate transporters were not saturated under our recording conditions. CTZ did not alter the amplitude or time course of the glutamate transporter currents (n = 7), nor did it change the paired-pulse ratio ($p > 0.05$), implying that CTZ lacked significant effects on the magnitude or kinetics of transmitter release.

Experiments in outside-out patches (**Fig. 3b**) confirmed that CTZ enhanced the activation of AMPAR currents at low glutamate concentrations[28]. Pulses of 100 μM glutamate evoked AMPAR currents whose rise times tracked the duration of the glutamate transient, in contrast with millimolar glutamate[35]. As the glutamate pulse was prolonged (from 1 to 5.5 ms), the 10–90% rise time for control AMPA current increased from 0.80 ± 0.05 ms to 3.5 ± 0.5 ms (n = 5), and from 0.83 ± 0.05 ms to 3.93 ± 0.15 ms in CTZ (n = 4). Thus, CTZ would be expected to unmask slowly rising AMPAR responses if $[glu]_{cleft}$ gradually rose to a low peak concentration.

This prediction was tested at silent synapses that showed failures in nearly all trials at hyperpolarized potentials, but not at depolarized potentials (**Fig. 4a**). The application of CTZ (100 μM) revealed an abundance of synaptic responses at negative potentials. As expected for AMPAR-mediated events, these responses were completely eliminated by CNQX (**Fig. 4b**). The CTZ-enhanced synaptic currents rose slowly (average 10–90% rise time, 4.1 ± 0.3 ms, n = 9), as expected if $[glu]_{cleft}$ reached low levels but persisted for several milliseconds (**Fig. 3b**). The slowness of the AMPAR currents could not be readily accounted for by

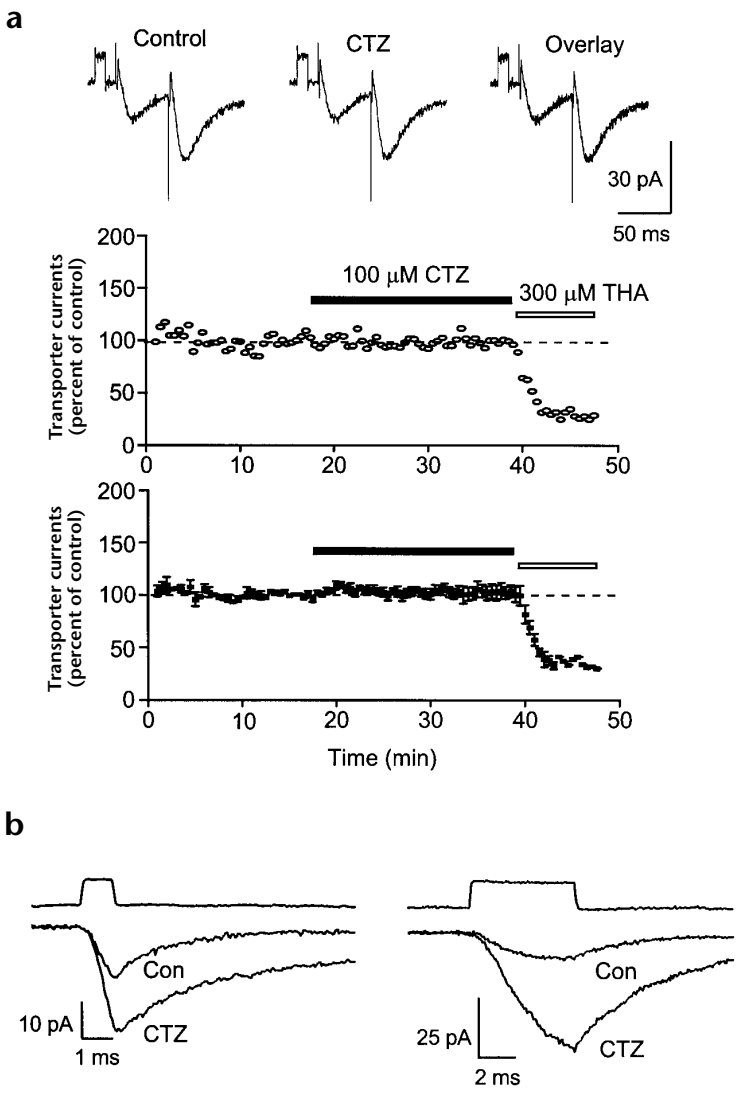

Fig. 3. CTZ does not alter glutamate transporter currents recorded from astrocytes in stratum radiatum of area CA1, but enhances AMPA receptor function. (**a**, top) Glutamate transporter currents shown before (control) and after 100 μM CTZ (CTZ). Paired stimuli were separated by 50 ms and produced paired-pulse facilitation. The PPF ratio was unchanged by exposure to CTZ (1.74 ± 0.10 in control and 1.66 ± 0.11 in CTZ, $p > 0.09$). (**a**, middle) Continuous monitoring of glutamate transporter currents over time in the same experiment. (**a**, bottom) Averaged data from seven experiments. Glial cell currents were inhibited by 300 μM THA, an antagonist of glutamate transporters. (**b**) CTZ potentiates glutamate responses of outside-out membrane patches from CA1 neurons. AMPAR current responses of outside-out patches to 1-ms (left) or 5.5-ms (right) pulses of 100 μM glutamate. In pooled data, 100 μM CTZ enhanced the responses by 2.28 ± 0.29-fold and 3.78 ± 0.38-fold, respectively.

increased detection of distal dendritic inputs shaped by cable filtering. The voltage-clamp conditions were optimized and stable (Methods), and the unitary synaptic currents were extremely small. Furthermore, the rise times of the CTZ-enhanced synaptic currents lacked significant correlation with decay times ($p = 0.73 \pm 0.1$, $n = 9$), as would be expected if dendritic filtering were predominant[36].

Having found that slowly rising EPSCs could be unmasked by CTZ at largely 'silent' synapses, we looked more closely at changes in AMPAR responses during potentiation in the presence of CTZ. If LTP were associated with enhancement of the speed and magnitude of the rise in $[glu]_{cleft}$, the slowly rising EPSCs should be converted to rapidly rising events. Hippocampal slices were pre-exposed to 100 μM CTZ for over 15 minutes before recording, and the effects of pairing were examined at minimally stimulated synapses showing very small, slowly rising EPSCs (**Fig. 5**). As predicted, the rise times of these EPSCs were significantly reduced with pairing-induced potentiation in the continued presence of CTZ in all 7 cells, decreasing from 4.1 ± 0.6 ms before pairing to 1.8 ± 0.2 ms after LTP ($p < 0.01$). In 6 of 7 cells, the decay time was also modified by pairing, increasing from 6.8 ± 0.5 ms before pairing to 10.5 ± 1.1 ms after LTP ($p < 0.02$). In contrast, we failed to observe a significant change in failure rate after pairing in any of the recordings (**Fig. 5d**, $p > 0.4$), consistent with the idea that individual presynaptic terminals already active before pairing were not subject to further recruitment. The pairing-induced slowing of AMPA EPSC decay makes sense in light of previous studies. Simulations of synaptic events with AMPAR desensitization removed suggest that low concentrations of glutamate are cleared more rapidly than high concentrations, thereby causing corresponding differences in EPSC decay rate[37]. Furthermore, evidence for a tetrameric structure of the AMPA receptor[27] supports the prediction that the transition of AMPARs from activated to resting states will take longer for higher initial occupancy of the four glutamate-binding sites.

Discussion

Our findings provide a new perspective on mechanisms of pairing-induced potentiation in young hippocampal slices. Before pairing, peak cleft glutamate concentration at silent synapses fell well short of 170 μM, low enough to allow complete inhibition of NMDAR EPSCs by 250 μM L-AP5 and to escape clear detection by postsynaptic AMPARs. However, the existence of functional AMPARs and CNQX-sensitive transmission was revealed by administration of CTZ (with no discernible presynaptic effects). After potentiation, peak $[glu]_{cleft}$ reached millimolar values, thus yielding NMDAR responses that were only partially blocked by 250 μM L-AP5 and clearly detectable transmission via AMPARs. In the continuing presence of CTZ, potentiation was manifested by a conversion of slowly rising, rapidly falling events to relatively rapidly rising, slowly falling ones. The striking change in the peak magnitude and time course of $[glu]_{cleft}$ was inconsistent with modification of glutamate transporters or buffers[26], but instead implied some sort of presynaptic modification. The demonstration of presynaptic modifications does not conflict with the possibility that functional AMPA receptors were recruited at postsynaptic sites[8]. The CTZ-enhanced, CNQX-sensitive responses would be compatible with recruitment of functional AMPARs, provided that the basal density of AMPARs were significantly different from zero. Several presynaptic scenarios may be considered as candidate mechanisms.

Vesicular filling state

If the degree of filling of synaptic vesicles were changed as a result of potentiation, peak $[glu]_{cleft}$ would also vary accord-

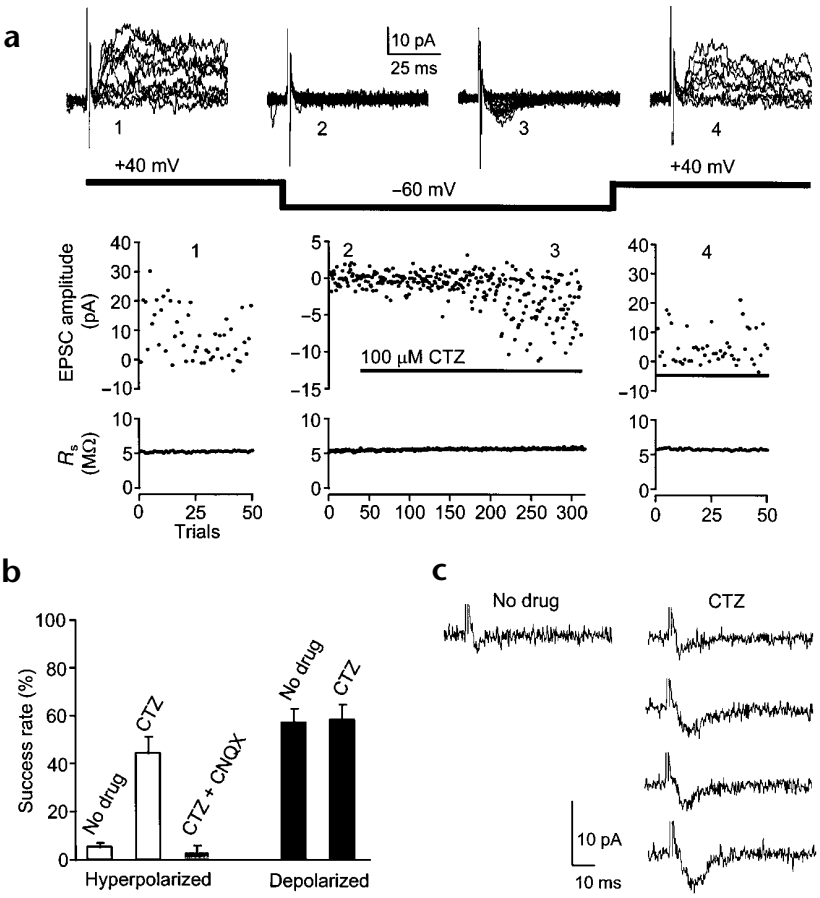

Fig. 4. Potentiation of receptor function by CTZ revealed small, often slowly rising AMPAR-mediated synaptic responses from silent synapses. (**a**) Representative experiment. Synaptic transmission was elicited at a frequency of 0.33 Hz without interruption. Groups of consecutive current records taken before (1, 2) and after (3, 4) exposure to CTZ. Amplitudes at +40 mV were assessed 35 ms after the stimulus; those at –60 mV were measured 9 ms after the stimulus. (**b**) Summary of 9 experiments showing that CTZ increased the success rate monitored at negative potentials (14.4 ± 2.9% and 48.4 ± 6.3% before and during CTZ exposure, $p < 0.0005$), but not at depolarized potentials (55.4 ± 9.1% and 53.7 ± 9.3% before and during exposure to CTZ, respectively, $p > 0.4$). Note that 10 μM CNQX completely inhibited CTZ-induced EPSCs from silent synapses. Based on lack of change in NMDA failures, we saw no presynaptic effects of CTZ under our experimental conditions, confirming the result obtained with glial cell recording (**Fig. 3**). The proportion of synaptic failures was estimated by doubling the fraction of responses with less-than-zero amplitude[4]. (**c**) Representative current traces before and during exposure to CTZ from the experiment shown in (**a**), displayed individually.

ingly[38]. However, this interpretation seems incompatible with the kinetic data. The discharge of neurotransmitter from a partially filled vesicle would be at least as fast as that from a completely filled vesicle, in contradiction to the changes in time course of $[glu]_{cleft}$ inferred from recordings of slowly rising, CTZ-enhanced AMPAR currents at silent synapses.

Glutamate spillover

It is proposed that NMDA-only transmission reflects spillover of glutamate from neighboring boutons in the face of failures of transmitter release at the immediately presynaptic terminal[16]. However, we found no increase in the incidence of NMDA successes after pairing (**Fig. 2**), excluding a significant increase in the probability of release from the immediately presynaptic terminal as the spillover hypothesis would require[16]. Our experiments were well suited to detect such an effect, as the incidences of NMDAR failures or successes were roughly equal. The potentiation of CTZ-enhanced AMPAR responses was associated with a slowing of decay time (**Fig. 5**), not the acceleration expected if spillover had been supplanted by immediately presynaptic release[39]. Thus, our data do not support a spillover scenario, although we cannot rule it out. It is possible that spillover may be more pronounced with massive tetanic stimulation than with the minimal stimulation used in this study.

Changes in properties of presynaptic fusion pores

How could a small but slow $[glu]_{cleft}$ transient be generated by presynaptic terminals immediately apposed to the postsynaptic neuron? We propose that the slow release arises from a vesicular-fusion pore that operates in a nonexpanding mode under baseline conditions and converts to a rapidly expanding mode upon establishment of LTP. Both of these modes of operation of fusion pores are found in amperometric recordings of secretion from invertebrate neurons[17] and non-neuronal cells[18–20]. Protein kinase C can sharply increase the rate of fusion-pore expansion[40], which is implicated in LTP[41]. A change in the mode of gating of presynaptic fusion pores represents a precisely targeted, switch-like action for which there is ample precedent in secretory cells. It would provide an explanation for previous data indicating decreased incidence of AMPAR failures[25,42], greater frequency of spontaneous AMPAR events[43] and increased uptake of presynaptic markers[9–11]. Regulation of peak $[glu]_{cleft}$ by modulation of presynaptic fusion pores offers significant functional advantages for both synaptic plasticity and development. The proposed mechanism would allow extremely local, NMDAR-only transmission in the basal state, thus maximizing the input specificity of Hebb's rule, and would also support efficient, stepwise increases in AMPAR transmission upon potentiation.

Methods

Slice preparation. 'Silent synapses' were studied in slices from 2–8-d old rats, in which such synapses are prominent[6]. After decapitation, brains were cooled in ice-cold, modified aCSF containing 194 mM sucrose, 20 mM NaCl, 3.5 mM KCl, 1.3 mM $MgCl_2$, 1.25 mM NaH_2PO_4, 26 mM $NaHCO_3$ and 11 mM glucose, gassed with 95% O_2/5% CO_2 at room temperature. Transverse hippocampal slices (300 μm) were cut in ice-cold modified aCSF using a vibroslicer. Slices were submerged in the recording chamber and superfused continuously (2–4 ml per min) with aCSF containing 120 mM NaCl, 3.5 mM KCl, 1.3 mM $MgCl_2$, 2 mM $CaCl_2$, 1.25 mM NaH_2PO_4, 26 mM $NaHCO_3$, 11 mM glucose and 0.1 mM picrotoxin, and gassed with 95% O_2/5% CO_2 at room temperature. A cut was made between regions CA3 and CA1 to prevent epileptiform activity.

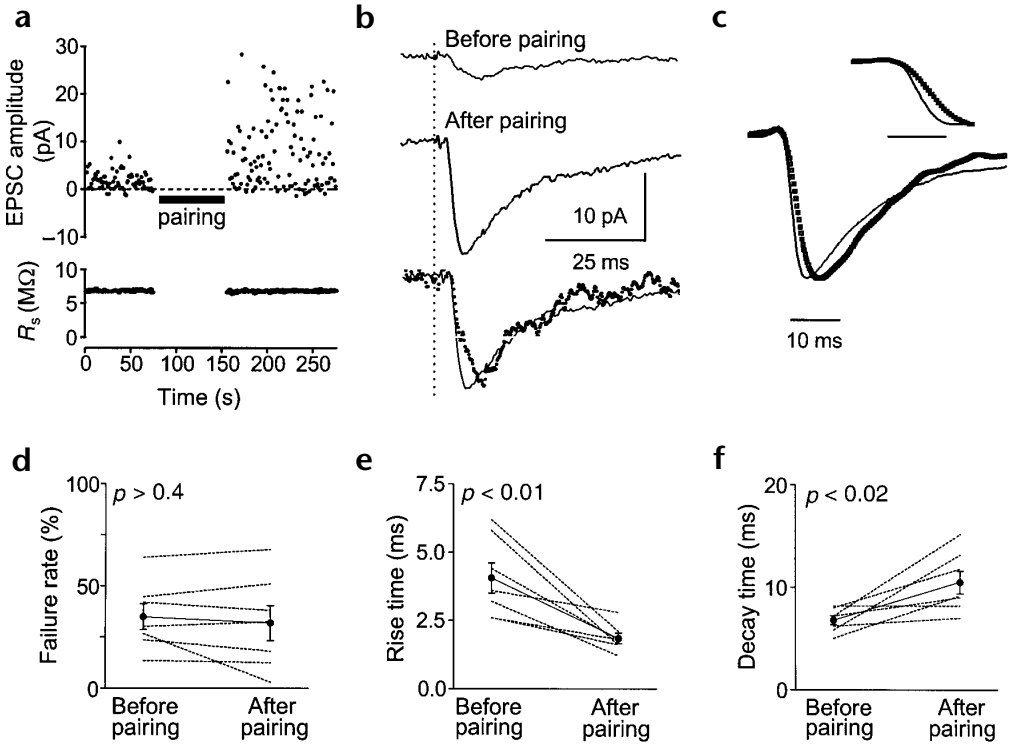

Fig. 5. In the presence of CTZ, pairing-induced potentiation altered EPSC kinetics. (**a**) Representative experiment demonstrating potentiation in the presence of 100 μM CTZ. (**b**) Averaged current traces from the same experiment, collected before and after pairing. EPSCs >3.5-fold larger than the standard deviation of the background noise were aligned and averaged. Stimulus artifacts nullified by subtraction of an average of current traces judged by eye as failures. The vertical dotted line indicates the start of stimulation. Superimposed traces at the bottom are the same averaged currents as above, normalized to the same peak amplitude (dotted trace, before pairing; continuous line, after pairing). (**c**) Grand average of current signals of the kind shown in (**b**) from seven individual experiments. Dotted trace and continuous line represent grand averages before and after pairing, respectively. For the grand mean, averaged, normalized traces from individual experiments were aligned based on the starts of their rising phases. (**c**, inset) Expanded display of the rising phase (horizontal scale bar, 5 ms). Average degree of potentiation upon pairing was 601 ± 242% (n = 7). CNQX completely inhibited synaptic responses after pairing in two of two cells tested. (**d–f**) Summary of seven experiments comparing synaptic properties before and after pairing. (**d**) Pairing produced no significant change of failure rate (before, 34.9 ± 6.3%; after, 31.8 ± 8.6%; $p > 0.4$). Pairing significantly decreased the 10–90%-rise time (**e**) and significantly increased the 90–50%-decay time (**f**).

Whole-cell voltage-clamp recordings. Recordings from CA1 pyramidal neurons 3–4 cell layers below the slice surface were made under DIC at 22°C. Synaptic transmission was elicited at 0.3–0.5 Hz with monopolar stimulating electrodes, positioned on stratum radiatum within 100 μm from stratum pyramidale. EPSCs were recorded with a patch electrode (1–4 MΩ tip resistance, no fire polishing or Sylgard coating) in whole-cell recording mode (Axopatch-1D). Pipet solution contained 100 mM Cs-gluconate, 0.6 or 10 mM EGTA, 10 mM HEPES, 10 mM CsCl, 5 mM NaCl, 20 mM TEA-OH, 4 mM Mg-ATP and 0.3 mM Na-GTP (raised to pH 7.3 with CsOH). The series resistance was not compensated but was monitored continuously using a 2-mV voltage pulse and averaged 7.3 ± 0.3 MΩ (n = 52). Recordings showing >20% change in series resistance were discarded. We implemented minimal stimulation, only slightly greater than the strongest stimulus that consistently yielded failures, although there was no certainty of stimulating a single input axon. We used recordings showing a uniform onset latency and a relatively constant potency of EPSCs. Inputs were considered to be silent when 25–50 successive failures of AMPAR responses were observed at a negative holding potential following observation of outward NMDA EPSCs at a 40–50% success rate for the same input. Stimulation frequency was maintained constant without interruption throughout the entire experiment, unless otherwise noted. LTP was induced by pairing of stimulation of afferent presynaptic fibers (50–100 stimuli) with postsynaptic depolarization (to 0 mV).

Outside-out patch recordings and ultrafast solution changes. We recorded from patches taken from somata of CA1 pyramidal cells in slices from 5–8 d-old rats. External solutions were gravity-fed to each lumen of theta glass tubing pulled to a tip diameter of ~200 μm. Fast solution changes (10–90% rise time <200 μs) were elicited by rapid movement of the interface between solutions, driven by a piezoelectric translator (LSS-3100, Burleigh, Fisher, New York). For NMDA currents, control external solution contained 160 mM NaCl, 2.5 mM KCl, 1 mM $CaCl_2$, 10 mM HEPES, 10 μM glycine, 2 μM CNQX (disodium salt), 2 μM picrotoxin and 1 μM tetrodotoxin at pH 7.3. To record AMPAR currents, glycine and CNQX were removed and 2 mM $MgCl_2$ and 50 μM D-AP5 were added. Internal solution contained 150 mM CsCl, 10 mM HEPES and 10 mM EGTA at pH 7.2.

Recordings of glutamate transporter currents. Recordings were made from astrocytes in stratum radiatum at 22°C with aCSF containing 1.5–2 mM $CaCl_2$ in hippocampal slices prepared from 5–8-d old rats as described[34]. A cut was made between regions CA3 and CA1. The recording solution included 10 μM CNQX, 100 μM D-AP5 and 100 μM picrotoxin. Whole-cell electrodes (2–4 MΩ) were filled with 120 mM potassium methylsulfate, 10 mM EGTA, 20 mM HEPES, 2 mM Mg-ATP and 0.2 mM Na-GTP at pH 7.4. Astrocytes identified by small cell bodies, low input resistance and high resting potentials (–91.5 ± 2.0 mV, n = 7) were subsequently held at resting potential. Schaffer collateral-commissural fibers were stimulated with a bipolar stimulating electrode in stratum radiatum (pulses of 50–150 μA and 100 μs, delivered at 0.05 or 0.1 Hz).

Data acquisition and analysis. EPSCs were filtered at 1–2 kHz, digitized at 5 kHz and stored. Amplitudes of AMPAR-mediated EPSCs recorded at –60 to –90 mV were determined by averaging the current over a 1-ms window centered on the peak response and subtracting a baseline estimate from the same record. The stimulus artifact was subtracted using an average of visually identified failures. Amplitudes of NMDAR-mediated EPSCs (+40 mV) were estimated by averaging the current over a 5–10-ms window 30–40 ms after the peak and subtracting a baseline estimate from the same record. Precise control of the duration of the antag-

onist exposure was achieved by means of a three-way stopcock that produced a sharply defined change in superfusing solutions. To gauge failure rate or degree of antagonist inhibition, the same number of EPSCs were collected just before beginning and ending antagonist application. All parameters for such determinations were kept constant for repeated antagonist applications in a given experiment. Averaged values are given as mean ± s.e. and were compared statistically by paired *t*-test (criterion for significance, $p < 0.05$), unless otherwise noted.

Acknowledgements

This work was supported by the Silvio Conte-NIMH Center for Neuroscience Research at Stanford (R.W.T.), a Dean's Fellowship (S.C.) and a fellowship of the Boehringer Ingelheim Fonds (J.K.). We thank D.V. Madison and P. Mermelstein for comments on the manuscript, N. C. Harata and E. T. Kavalali for discussions and D. Wheeler and D. Profitt for technical support. We are grateful to other members of the Tsien lab for their support.

RECEIVED 25 OCTOBER 1999; ACCEPTED 10 FEBRUARY 2000

1. Bliss T. V. P. & Collingridge G. L. A synaptic model of memory: long-term potentiation in the hippocampus. *Nature* **361**, 31–39 (1993).
2. Kullmann, D. M. & Siegelbaum, S. A. The site of expression of NMDA receptor-dependent LTP: new fuel for an old fire. *Neuron* **15**, 997–1002 (1995).
3. Malenka, R. C. & Nicoll, R. A. Long-term potentiation—a decade of progress? *Science* **285**, 1870–1874 (1999).
4. Liao, D., Hessler, N. A. & Malinow, R. Activation of postsynaptically silent synapses during pairing-induced LTP in CA1 region of hippocampal slice. *Nature* **375**, 400–404 (1995).
5. Isaac, J. T., Nicoll, R. A. & Malenka, R. C. Evidence for silent synapses: implications for the expression of LTP. *Neuron* **15**, 427–434 (1995).
6. Durand, G. M., Kovalchuk, Y. & Konnerth, A. Long-term potentiation and functional synapse induction in developing hippocampus. *Nature* **381**, 71–75 (1996).
7. Nüsser, Z. *et al.* Cell type and pathway dependence of synaptic AMPA receptor number and variability in the hippocampus. *Neuron* **21**, 545–559 (1998).
8. Shi, S. H. *et al.* Rapid spine delivery and redistribution of AMPA receptors after synaptic NMDA receptor activation. *Science* **284**, 1811–1816 (1999).
9. Malgaroli, A. *et al.* Presynaptic component of long-term potentiation visualized at individual hippocampal synapses. *Science* **268**, 1624–1628 (1995).
10. Ryan, T. A., Ziv, N. E. & Smith, S. J. Potentiation of evoked vesicle turnover at individually resolved synaptic boutons. *Neuron* **17**, 125–134 (1996).
11. Ma, L., Zablow, L., Kandel, E. R. & Siegelbaum, S. A. Cyclic AMP induces functional presynaptic boutons in hippocampal CA3–CA1 neuronal cultures. *Nat. Neurosci.* **2**, 24–30 (1999).
12. Patneau, D. K. & Mayer, M. L. Structure-activity relationships for amino acid transmitter candidates acting at N-methyl-D-asartate and quisqualate receptors. *J. Neurosci.* **10**, 2385–2399 (1990).
13. Perkel, D. J. & Nicoll, R. A. Evidence of all-or-none regulation of neurotransmitter release: implications for long-term potentiation. *J. Physiol. (Lond.)* **471**, 481–500.
14. Kullmann, D. M. Excitatory synapses. Neither too loud nor too quiet. *Nature* **13**, 111–112 (1999).
15. Clements, J. D., Lester, R. A., Tong, G., Jahr, C. E. & Westbrook, G. L. The time course of glutamate in the synaptic cleft. *Science* **258**, 1498–1501 (1992).
16. Kullmann, D. M. & Asztely, F. Extrasynaptic glutamate spillover in the hippocampus: evidence and implications. *Trends Neurosci.* **21**, 8–14 (1998).
17. Bruns, D. & Jahn, R. Real-time measurement of transmitter release from single synaptic vesicles. *Nature* **377**, 62–65 (1995).
18. Zhou, Z, Misler, S. & Chow, R. H. Rapid fluctuations in transmitter release from single vesicles in bovine adrenal chromaffin cells. *Biophys. J.* **70**, 1543–1552 (1996).
19. Spruce, A. E., Breckenridge, L. J., Lee, A. K. & Almers, W. Properties of the fusion pore that forms during exocytosis of a mast cell secretory vesicle. *Neuron* **4**, 643–654 (1990).
20. Lollike, K., Borregaard, N. & Lindau, M. Capacitance flickers and pseudoflickers of small granules, measured in the cell-attached configuration. *Biophys. J.* **75**, 53–59 (1998).
21. Tong, G. & Jahr, C. E. Multivesicular release from excitatory synapses of cultured hippocampal neurons. *Neuron* **12**, 51–59 (1994).
22. Clements, J. D. Transmitter timecourse in the synaptic cleft: its role in central synaptic function. *Trends Neurosci.* **19**, 163–171 (1996).
23. Olverman, H. J., Jones, A. W., Mewett, K. N. & Watkins, J. C. Structure/activity relations of N-methyl-D-aspartate receptor ligands as studied by their inhibition of [^{3}H]D-2–amino-5–phosphonopentanoic acid binding in rat brain membranes. *Neuroscience* **26**, 17–31 (1988).
24. Rumpel, S., Hatt, H. & Gottmann, K. Silent synapses in the developing rat visual cortex: evidence for postsynaptic expression of synaptic plasticity. *J. Neurosci.* **18**, 8863–8874 (1998).
25. Malinow, R. & Tsien, R. W. Presynaptic enhancement shown by whole-cell recordings of long-term potentiation in hippocampal slices. *Nature* **346**, 177–180 (1990).
26. Diamond, J. S. & Jahr, C. E. Transporters buffer synaptically released glutamate on a submillisecond time scale. *J. Neurosci.* **17**, 4672–4687 (1997).
27. Rosenmund, C., Stern-Bach, Y. & Stevens, C. F. The tetrameric structure of a glutamate receptor channel. *Science* **280**, 1596–1599 (1998).
28. Dzubay, J. A. & Jahr, C. E. The concentration of synaptically released glutamate outside of the climbing fiber-purkinje cell synaptic cleft. *J. Neurosci.* **19**, 5265–5274 (1999).
29. Partin, K. M., Patneau, D. K., Winters, C. A., Mayer, M. L. & Buonanno, A. Selective modulation of desensitization at AMPA versus kainate receptors by cyclothiazide and concanavalin A. *Neuron* **11**, 1069–1082 (1993).
30. Yamada, K. A. & Tang, C. M Benzothiadiazides inhibit rapid glutamate receptor desensitization and enhance glutamatergic synaptic currents. *J. Neurosci.* **13**, 3904–3915 (1993).
31. Diamond, J. S. & Jahr, C. E. Asynchronous release of synaptic vesicles determines the time course of the AMPA receptor-mediated EPSC. *Neuron* **15**, 1097–1107 (1995).
32. Bellingham, M. C. & Walmsley, B. A novel presynaptic inhibitory mechanism underlies paired pulse depression at a fast central synapse. *Neuron* **23**, 159–170 (1999).
33. Lüscher, C. Malenka, R. C. & Nicoll, R. A. Monitoring glutamate release during LTP with glial transporter currents. *Neuron* **21**, 435–441 (1998).
34. Diamond, J. S., Bergles, D. E. & Jahr, C. E. Glutamate release monitored with astrocyte transporter currents during LTP. *Neuron* **21**, 425–433 (1998).
35. Colquhoun, D., Jonas, P. & Sakmann, B. Action of brief pulses of glutamate on AMPA/kainate receptors in patches from different neurones of rat hippocampal slices. *J. Physiol. (Lond.)* **458**, 261–287 (1992).
36. Bekkers, J. M. & Stevens, C. F. Cable properties of cultured hippocampal neurons determined from sucrose-evoked miniature EPSCs. *J. Neurophysiol.* **75**, 1250–1255 (1996).
37. Glavinovic M. I. & Rabie, H. R. Monte Carlo simulation of spontaneous miniature excitatory postsynaptic currents in rat hippocampal synapse in the presence and absence of desensitization. *Pflugers Arch.* **435**, 193–202 (1998).
38. Pothos, E. N., Przedborski, S., Davila, V., Schmitz, Y. & Sulzer, D. D2-like dopamine autoreceptor activation reduces quantal size in PC12 cells. *J. Neurosci.* **18**, 4106–4118 (1998).
39. Rossi, D. J. & Hamann, M. Spillover-mediated transmission at inhibitory synapses promoted by high affinity alpha6 subunit GABA(A) receptors and glomerular geometry. *Neuron* **20**, 783–795 (1998).
40. Scepek, S., Coorssen, J. R. & Lindau, M. Fusion pore expansion in horse eosinophils is modulated by Ca^{2+} and protein kinase C via distinct mechanisms. *EMBO J.* **17**, 4340–4346 (1998).
41. Malinow, R., Schulman, H. & Tsien, R. W. Inhibition of postsynaptic PKC or CaMKII blocks induction but not expression of LTP. *Science* **245**, 862–866 (1989).
42. Bekkers, J. M. & Stevens, C. F. Presynaptic mechanism for long-term potentiation in the hippocampus. *Nature* **346**, 724–729 (1990).
43. Malgaroli, A & Tsien, R. W. Glutamate-induced long-term potentiation of the frequency of miniature synaptic currents in cultured hippocampal neurons. *Nature* **357**, 134–139 (1992).